# Secondary ion mass spectrometer analyses for trace elements in glass standards using variably charged silicon ions for normalization

ERIC N. CARLSON<sup>1,‡</sup> AND RICHARD L. HERVIG<sup>1,\*,†</sup>

<sup>1</sup>School of Earth and Space Exploration, Arizona State University, Tempe, Arizona 85287, U.S.A.

#### ABSTRACT

Trace element analyses of silicate materials by secondary ion mass spectrometry (SIMS) typically normalize the secondary ion count rate for the isotopes of interest to the count rate for one of the silicon isotopes. While the great majority of SIMS analyses use the signal from Si<sup>+</sup>, some laboratories have used a multiply charged ion (Si<sup>2+</sup> or Si<sup>3+</sup>). We collected data and constructed calibration curves for lithium, beryllium, and boron using these different normalizing species on synthetic basaltic glass and soda-lime silicate glass standards. The calibrations showed little effect of changing matrix when Si<sup>+</sup> was used, but larger effects (up to a factor of ~2) when using Si<sup>2+</sup> or Si<sup>3+</sup> are a warning that care must be taken to avoid inaccurate analyses. The smallest matrix effects were observed at maximum transmission compared to detecting ions with a few tens of eV of initial kinetic energy ("conventional energy filtering"). Normalizing the light element ion intensities to Al<sup>3+</sup> showed a smaller matrix effect than multiply-charged Si ions. When normalized to  $^{16}O^+$  (which includes oxygen from the sample and from the primary beam), the two matrices showed distinct calibration curves, suggesting that changing sputter yields (atoms ejected per primary atom impact) may play a role in the probability of producing multiply charged silicon ions.

Keywords: SIMS, lithium, beryllium, boron; Lithium, Beryllium and Boron: Quintessentially Crustal

## Introduction

Secondary ion mass spectrometry (SIMS) is very sensitive to many elements, and the three light lithophile elements, lithium, beryllium, and boron, have represented a frequent application of this technique. There are many examples of the calibration of SIMS for these elements (e.g., Hervig 1996, 2002; Ottolini et al. 1993). These reports indicate that the variation in major element chemistry does not play a large role in changing the calibration factor (e.g., Ottolini et al. 1993; Dunham et al. 2020), although there are exceptions (de Hoog and EIMF 2018). That is, the effect of bulk chemistry on the ion yield of these elements at trace levels in "common" matrices tends to be small. Most SIMS calibrations involve normalizing the intensity of the ion of interest to a matrix ion, such as one of the silicon isotopes, when studying silicate minerals and glasses. The normalization is important because (at least in the Cameca IMS design) there is a very strong potential gradient between the sample and the grounded extraction lens, and if the distance between the sample and ground varies (resulting from using even slightly tilted samples or slightly deformed sample holders), the absolute count rates can change, while ion ratios (e.g., Li<sup>+</sup>/Si<sup>+</sup>) will vary less as the sample is moved to examine different areas [note that even the ion ratios may be significantly affected if tilting is excessive (Deng and Williams 1989)].

Some published results select secondary ions ejected with

several tens of eV initial kinetic energy [the energy filtering approach (e.g., Shimizu and Hart 1982; de Hoog and EIMF 2018)] while other researchers have used the more intense, low-energy secondary ions (e.g., Marschall and Monteleone 2014; Dunham et al. 2020). In these and in most other applications to geological materials, the normalizing ion was typically singly charged silicon. However, silicon (like many other elements) will form multiply charged ions (such as Si<sup>2+</sup>, Si<sup>3+</sup>, and even Si<sup>4+</sup>), for which the signal shows up at mass/charge of 14, 9.3, and 7, assuming the most abundant isotope, <sup>28</sup>Si, is detected. One attraction of using, for example, the doubly charged ion is that the count rate decreases by a factor of a few thousand compared to the singly charged ion, allowing the operator to increase the primary beam current to remove more atoms of trace elements/isotopes and increase sensitivity while keeping the normalizing ion from saturating the electron multiplier (EM) detector. Using a different detector for Si (Faraday cup) than the trace elements in the analysis routine (electron multiplier) is an alternative, but might affect precision because of changing EM detector parameters (aging). Perhaps the most important reason to explore the effects of using multiply charged ions is that applications to light element (Li to B elemental and isotopic) analysis using large-geometry SIMS instruments typically involve collecting a signal for silicon using Si3+ or Si2+. This requires a smaller change in the magnetic field compared to monitoring singly charged silicon (see, for example, Dunham et al. 2020), thus reducing hysteresis effects on instruments with large magnets.

There is nothing intrinsically wrong with using multiply charged ions in SIMS analyses. For example, Riciputi et al. (1993) asserted that calibrations for rare earth elements using

<sup>\*</sup> E-mail: hervig@asu.edu

<sup>†</sup> Present address: PO Box 663, Santa Cruz, New Mexico 87567, U.S.A.

<sup>†</sup> Special collection papers can be found online at http://www.minsocam.org/MSA/ AmMin/special-collections.html.

doubly charged ions were robust. Ottolini (2002) used Ca<sup>2+</sup>/Si<sup>2+</sup> ion ratios to quantify the Ca content of olivine, and Harrison et al. (2010) used doubly charged ions to aid in determining the ages of feldspars using the <sup>40</sup>K-<sup>40</sup>Ca decay system. Doubly charged ions have been used to help understand the sputtering process itself (e.g., Schauer and Williams 1992; Franzreb et al. 2004).

However, the use of multiply charged ions could have drawbacks. For example, if one places a potential of 10000 V on the sample, singly charged ions are accelerated to 10 keV energies (plus any energy resulting from the collision cascade), whereas doubly and triply charged ions will be accelerated to 20 and 30 keV energies (and thus greater velocities), respectively. Because the probability of generating a pulse on the electron multiplier generally scales with ion velocity (Zinner et al. 1986), the relatively faster, multiply charged ions will be more efficiently detected than singly charged ions of the same element. Depending on the number of multiply charged ions striking the electron multiplier (e.g., if one monitors Si<sup>2+</sup> intensities while waiting for the secondary ion signal to stabilize), accelerated aging of this detector is conceivable. Degraded reproducibility on standards when using multiply charged silicon compared to normalizing to the singly charged species stopped the ASU SIMS lab from using Si<sup>2+</sup> in the early 1990s (ASU lab, unpublished data). Another consideration is whether the process that generates multiply charged ions is similar to that which generates singly charged ions. Schauer and Williams (1992) showed that not only are the energy spectra of 1+ and 2+ ions from pure metals different, but their response to oxygen flooding is also different. The latter observation suggests that the yield of multiply charged ions may depend on the oxygen content of the sputtered crater floor and thus the relative abundance of singly and multiply charged species could depend on the particular sputtering conditions employed. In this contribution, we evaluate practical considerations of the use of singly and multiply charged ions in some trace element determinations by SIMS, in large part to point out some potential problems. We examine the effect of normalizing the intensity of Li<sup>+</sup>, Be<sup>+</sup>, and B<sup>+</sup> sputtered from U.S. Geological Survey (GS) basaltic glass standards [GSA-, GSD-, and GSE-1G and NIST 610, 612, and 614 high-silica glass (Guillong et al. 2005; Jochum et al. 2005; Jochum et al. 2011)] to either Si<sup>+</sup>, Si<sup>2+</sup> or Si<sup>3+</sup> (as well as O<sup>+</sup> and Al<sup>3+</sup>) and describe changes in the resulting calibration curves as a function of matrix chemistry.

## ANALYTICAL METHODS

We used the Cameca IMS 6f SIMS at ASU for this work. The samples above were sputtered using a mass-filtered beam of 16O- or 16O2 formed in a modified Cameca duoplasmatron at a current of ~2-4 nA either rastered over a 10 × 10 μm<sup>2</sup> area or unrastered. Positive secondary ions were accelerated to either +5000 or +9000 V, and a combination of transfer optics and field apertures allowed ions to be collected from a 15 µm diameter circular area (including most of the sputtered crater). The energy window was set to allow ions with a ~40 eV range in energy into the mass spectrometer, and several sets of data were obtained in different sessions: (1) secondary ions with  $\sim 0 \pm 20$  eV initial kinetic energy along with  $Si^+$ ,  $Si^{2+}$ , and  $Si^{3+}$ ; (2) secondary ions with  $\sim 0 \pm 20$  eV and ions with  $-75 \pm 20$  eV initial kinetic energy along with Si+ and Si2+. On three occasions, intensities for <sup>16</sup>O<sup>+</sup> and <sup>27</sup>Al<sup>3+</sup> were also collected. All secondary ions were detected using an electron multiplier in pulse counting mode early in this project (including <sup>30</sup>Si<sup>+</sup>). A change in focus from examining 75 eV ions to 0 eV ions resulted in a decision to measure low-energy, singly charged <sup>28</sup>Si<sup>+</sup> on the secondary ion Faraday cup to avoid potential dead-time corrections on 30Si+. No difference in the results was observed between these later sessions and when low-energy 30Si+ was detected on

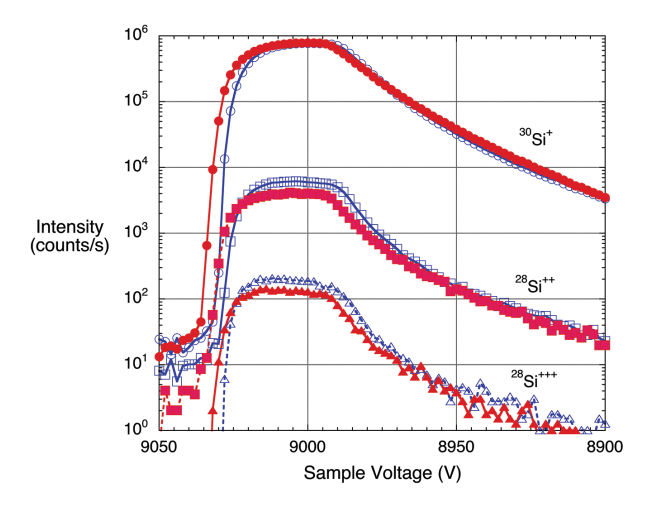


**FIGURE 1.** Energy spectra for singly, doubly, and triply charged silicon ions sputtered from NIST high-silica glass (open symbols) and GS basaltic glass (filled symbols). (Color online.)

the electron multiplier. The mass resolving power was set to either  $\sim\!800$  or  $\sim\!2000$  in different sessions. Counting times on the trace elements were sufficient to reach better than 10% statistical precision. Sample charging was examined by scanning the sample voltage while monitoring the count rate for a matrix ion on the EM and returning the sample voltage to give the peak count rate.

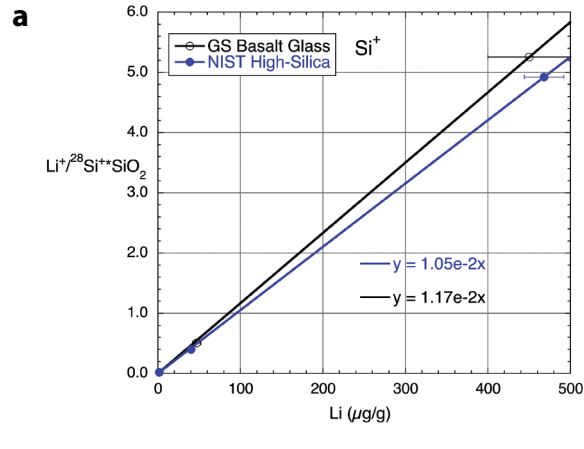
#### RESULTS

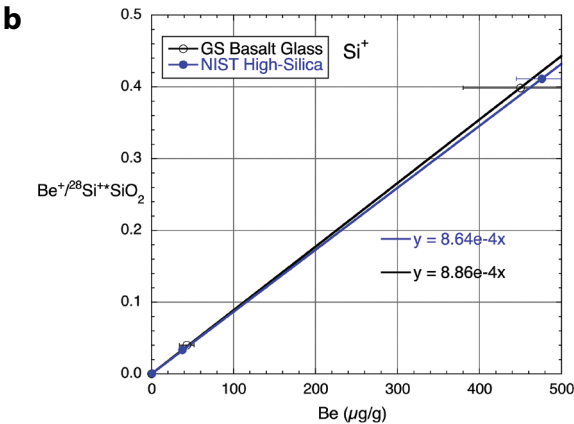
Primary ion impacts result in generating sputtered ions with a range of initial kinetic energies, and the energy spectra of <sup>30</sup>Si<sup>+</sup>, <sup>28</sup>Si<sup>2+</sup>, and <sup>28</sup>Si<sup>3+</sup> from NIST and GS glasses are shown in Figure 1. When the secondary ion count rates are examined on a log scale, the spectra show similar patterns, regardless of sample or species. We observe similar absolute count rates for Si<sup>+</sup> in both types of glass at a sample voltage of 9000 V (where most of the data were obtained). Even on a log scale, it is clear that the absolute intensities for Si<sup>2+</sup> and Si<sup>3+</sup> are lower for the basaltic glasses than the high-silica NIST glasses [note that the SiO<sub>2</sub> content of the soda-lime silicate base of NIST glasses is ~72 wt%, while the basaltic glasses contain 52–53 wt% (Jochum et al. 2005, 2011)].

We have compared calibration curves using the singly and multiply charged silicon ions for normalization. These curves are constructed by normalizing the M<sup>+</sup>/Si<sup>x+</sup> ion ratio to the silica abundance in the glass and comparing it with the concentration of the dopant, M. Linear calibrations are expected when the element of interest is at the trace or minor level. The slope of the line can be used to take the M<sup>+</sup>/Si<sup>x+</sup> ion ratio of an unknown sample and convert it to a concentration (after normalization to silica content).

As shown in Figure 2, the differences in calibration curves for Li, Be, and B between the U.S. Geological Survey basaltic glasses and the high-silica NIST 610 glass obtained in a typical analysis session are small. Considering the uncertainty in the concentrations of these elements, either regression could fit all the data in this session. Examination of Table 1 shows the range in the slopes of these calibration curves over several sessions. The worst-case is for Li and Be (up to a  $\sim$ 20% difference in calibration slopes), while the B calibrations on the two compositions are typically within  $\sim$ 10%.

Calibration curves similar to those in Figure 2 (obtained in the same session as those in Fig. 2) were constructed (Figs. 3 and





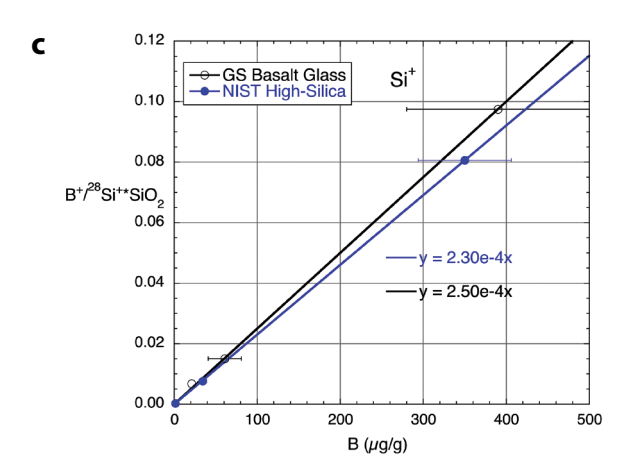


**FIGURE 2.** Calibration curves for  $^7\text{Li}$ ,  $^9\text{Be}$ , and  $^{11}\text{B}$ , using low-energy ions (0 ± 20 eV energy window) normalized to the count rate for  $^{28}\text{Si}^+$  and the SiO<sub>2</sub> content of the glass, either basaltic or in NIST 61X. The linear fits to the data are forced through the origin. (Color online.)

4). The difference in Figures 2, 3, and 4 is that the normalizing ion is  $Si^+$ ,  $Si^{2+}$ , and  $Si^{3+}$ , respectively. We observe that the NIST glasses are colinear, as are the Geological Survey glass samples. However, the linear regressions show distinctly different slopes. The difference in calibration factor (as indicated by the ratio of the slope for the basaltic glass/NIST glass) is a factor of 1.8 to 2 ( $Si^{2+}$ ) or 1.6 to 1.8 ( $Si^{3+}$ ) for all three elements (Table 2) over the

different analysis sessions (Tables 1 and 2). The slopes for the basaltic glasses are consistently higher than those for the high-silica NIST glasses.

Another set of calibration curves (Fig. 5) used Al<sup>3+</sup> as the normalizing ion. It can be observed that the basaltic glasses and the high-silica NIST glasses generate regression lines with more similar calibration factors (slopes) than when multiply charged silicon is used (see Tables 1 and 2), with the largest difference in slope around 20%. Again, the NIST glasses are colinear, as are the USGS basaltic glasses.

The secondary ion intensity for oxygen ( $^{16}O^{+}$ ) was collected in three analysis sessions, with the main purpose being to determine (and correct for) the extent of charging in the sputtered crater during the analysis, but we tested its use as a normalizing species in Figure 6. While the oxygen content of the basaltic glasses and the NIST glasses are similar ( $\sim$ 43 vs.  $\sim$ 46 wt%), the two compositions define different calibrations, with the basaltic glass consistently displaying a slope  $\sim$ 1.5× that of the NIST glasse. The NIST glasses are again colinear, as are the USGS basaltic compositions.

Because Schauer and Williams (1992) observed a difference in the energy spectra of doubly charged ions vs. singly charged ions, we also collected data at high energy (75  $\pm$  20 eV initial kinetic energy) to compare calibrations of M<sup>+</sup>/Si<sup>+</sup> with M<sup>+</sup>/Si<sup>++</sup> using conventional energy filtering (the Si<sup>+++</sup> signal intensity was too low to test this approach). As shown in Table 2, matrix effects between basaltic and high-silica glasses when normalizing to singly charged silicon show approximately the same magnitude as when low-energy secondary ions are used (Fig. 2), with a maximum dispersion in the calibration slopes <30%. When secondary ions with  $75 \pm 20$  eV initial kinetic energy are normalized to doubly charged silicon (Tables 1 and 2), the effect of the matrix is more pronounced, with beryllium and boron calibrations changing by a factor of 1.5 between basaltic glass and the high-silica NIST composition, although the measurements on lithium suggest a smaller effect.

The effect on calibration curves when using an elemental primary beam (<sup>16</sup>O<sup>-</sup>) vs. a molecular primary beam (<sup>16</sup>O<sub>2</sub>) was tested because of a suggestion by a thoughtful reviewer of this manuscript. During a session where both primary beams were used (see analyses obtained on 3 February 2022; Table 1), the results indicate that neither the NIST glass calibration nor the basaltic glass curves (when normalized to Si<sup>+</sup>) were affected by changing the primary species when boron is considered. A similar result was found (within 10%) for Be, and the largest effect of primary species (~20%) was observed for lithium (when dividing the calibration slope for O<sup>-</sup> by the calibration slope when using O<sub>2</sub> for a particular matrix). In addition, comparing the results obtained on the NIST and USGS glasses (Table 2) also suggests minimal differences related to selection of primary species—as in other sessions, the role of the normalizing element is observed to have a larger effect on the calibration curve than the selection of primary species.

#### DISCUSSION

The formation of doubly charged ions during sputtering has been suggested to arise via the ejection of a core electron. The transfer of a higher level electron to fill the core vacancy may release enough energy to eject a second valence electron, thus creating a doubly charged ion (see discussion in Schauer and 9/10/2019

11/5/2019

11/5/2019

6/29/2021

7/15/2021

7/16/2021

2/3/2022

2/3/2022

8925

5000

4425

9000

9000

9000

5000

5000

0

0-

 $O_{\bar{2}}$ 

 $O_{2}$ 

 $O_2^-$ 

0

Li+/Si+ Li<sup>+</sup>/Si<sup>+</sup> Li+/Al++ Li<sup>+</sup>/O<sup>+</sup> Li+/O+ Date Sample Primary Li+/Si Li+/Si+ NIST Species Basalt Basalt Basalt Basalt 9/10/2019 8925 0.00093 0.00068 N/A 0 0.94 1.05 N/A N/A N/A N/A N/A 11/5/2019 5000 0 0.0054 0.0050 N/A N/A N/A N/A N/A 3.2 4.8 N/A 0-0.77 11/5/2019 4425 0.00097 0.00069 0.92 N/A N/A N/A N/A N/A N/A 9000 N/A 6/29/2021  $O_{\bar{2}}$ N/A N/A N/A N/A N/A N/A N/A N/A N/A 7/15/2021 9000  $O_{\bar{2}}$ 0.0105 0.0116 40 80 1291 2286 466 599 0.023 0.035 7/16/2021 9000  $O_{\bar{2}}$ 0.0122 0.0103 43 61 1327 1772 486 484 0.026 0.032 2/3/2022 5000 0-0.0095 0.0114 12 19 371 456 150 150 0.037 0.053 2/3/2022 5000 0.0122 0.0146 86 167 2855 4972 836 1076 0.028 0.045 Be+/Si+ Be+/Si+ Be+/Si+ Be+/Si++ Be+/Si++ Be+/Si+++ Be+/AI+++ Be+/AI++ Be+/O+ Be+/O+ NIST Basalt NIST Basalt NIST Basalt NIST Basalt NIST Basalt 11/5/2019 5000 0 0.00072 0.00069 0.43 0.67 N/A N/A N/A N/A N/A N/A 11/5/2019 4425 0-N/A 0.00083 0.00080 0.67 1.06 N/A N/A N/A N/A N/A 9000  $O_2^-$ 0.00096 0.0025 0.0033 6/29/2021 0.00098 N/A N/A 142 186 48.7 50.8 7/15/2021 9000  $O_{\bar{2}}$ 0.00086 0.00089 3.32 6.05 106 174 383 45.6 0.0019 0.0027 0\_2 7/16/2021 9000 0.00095 0.00094 3.34 5.55 104 161 37.9 0.0020 0.0029 44 0-2/3/2022 5000 0.00076 0.00089 1.45 29.8 35.4 12.1 11.6 0.0030 0.0041 2/3/2022 5000 0.00082 0.00094 5.83 10.55 193 314 56 68 0.0019 0.0029 B+/Si+ B+/Si+ B+/Si++ B+/Si++ B+/Si++-B+/Si+++ B+/AI+++ B+/AI+++ B+/O+ B+/O+

TABLE 1. Slopes of calibration curves determined on NIST and GS glasses in different analysis sessions

Notes: Analysis sessions either detected ions with  $0\pm20$  eV initial kinetic energy (5000 or 9000 Sample V) or  $75\pm20$  eV initial kinetic energy (4425 or 8925 Sample V). Italics indicate three sessions where  $30Si^*$  was detected. Calibration curve slopes have been of  $^{28}Si$  ( $^{30}Si^*30 \sim ^{28}Si$ ) for comparison with other sessions.

Basalt

0.35

0.21

0.29

N/A

1.7

1.5

0.43

2.97

NIST

N/A

N/A

N/A

36

28

27

8.9

53.6

**Basalt** 

N/A

N/A

N/A

50

49

44

10.6

88.3

Williams 1992). If enough energy is released, more than one valence electron can be ejected, producing triply (or greater) charged ions (e.g., Slodzian 1975). While the energy spectrum of the ions sputtered from either high-silica or basaltic glasses appears similar (Fig. 1), a graph showing the ratio of the intensities of differently charged ions (now on a linear scale) as a function of sample voltage (Fig. 7) confirms the relatively low abundance of doubly and triply charged ions in the low-silica basaltic matrix compared to the NIST glass as well as the similar patterns for both glasses. Perhaps most importantly, the ratio of 2+/3+ ions from the two matrices shows a nearly overlapping trend as a function of sample voltage (Fig. 7), which may be support for the similar formation process suggested by Slodzian (1975).

NIST

0.00025

0.00021

0.00730

0.00025

0.00023

0.00025

0.00023

0.00023

**Basalt** 

0.00023

0.00022

0.00660

0.00026

0.00025

0.00026

0.00026

0.00026

NIST

0.25

0.13

0.19

N/A

0.9

0.9

0.30

1.62

Changing the sample chemistry clearly has an effect on the probability of forming multiply charged silicon ions. We suggest the relations in Figure 6 offer a possible reason. Nearly 90% of secondary atoms are derived from the top monolayer of the crater floor (Dumke et al. 1983), and the surface of the sample is most influenced by the addition of the primary beam. The concentration of the primary species in the surface is related to the sputter yield (atoms ejected per incident ion). The higher the sputter yield (the faster the sputtering rate), the less oxygen from the primary beam will build up in the sample surface. Thus, the relatively low-O+ ion intensity observed on the basaltic glasses suggests a higher sputter rate compared to the NIST high-silica glasses. This is intuitively sensible because the basaltic glasses contain higher mass elements (e.g., Fe) and, thus, higher stopping power. This leads to more surface and near-surface atoms being set in motion during primary ion impact, which increases the probability of their ejection. Increasing the oxygen content of the surface of pure Si tends to have very little effect on the probability of generating doubly charged ions (Schauer and Williams 1992), but the present data set may indicate that when more complex natural and synthetic glass compositions are examined, the O content of the crater floor varies, leading to changes in the ion yields of multiply charged silicon species.

NIST

N/A

N/A

N/A

12.2

10.2

9.9

3.6

15.7

Basalt

N/A

N/A

N/A

13.6

12.8

12

3.5

19.1

NIST

N/A

N/A

N/A

0.00064

0.00050

0.00052

0.00089

0.00053

Basalt

N/A

N/A

N/A

0.00089

0.00084

0.00079

0.00122

0.00080

Because the basaltic glasses show different calibration curves compared to high-silica NIST samples, while each composition displays colinear behavior (Figs. 3 and 4) when multiply charged silicon is used for normalizing purposes, it would be tempting to suggest that as long as the major element matrix is a good match, the calibration can be robustly applied to unknown materials. However, because natural glasses can contain significant (and variable) amounts of hydrogen, and the addition of H<sub>2</sub>O can have a large effect on sputter yield, and thus O content (e.g., Regier et al. 2016), caution is advised when using anhydrous standards and multiply charged Si ions to characterize hydrous unknowns using oxygen primary beams.

In contrast to using multiply charged Si ions for normalization, using triply charged aluminum ions shows a smaller change in sensitivity for the three light elements studied as the matrix changed (Fig. 6). Perhaps this relates to the propensity of Al atoms to efficiently getter oxygen so that the environment of surface Al in the two matrices is similar, but more research would be needed to explore this.

The impact energies (and thus the velocities) of the singly vs. multiply charged ions on the electron multiplier detector are very different, and we describe in the Introduction anecdotal information on larger-than-normal session-to-session variations in the calibration curves. While not emphasized in this study, we would suggest that electron multiplier parameters could be adjusted (mostly the gain) in each analysis session to optimize

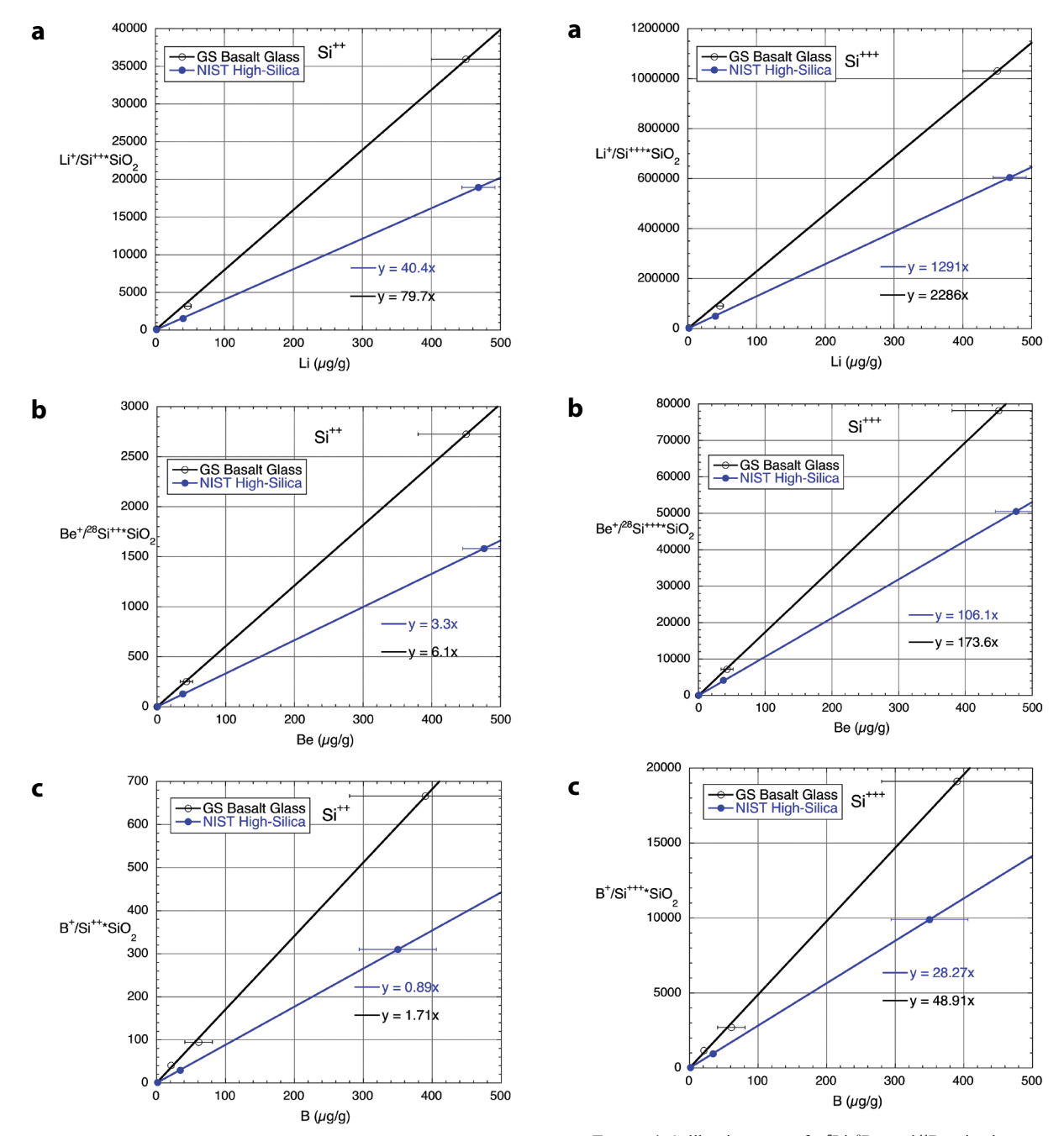


**FIGURE 3.** Calibration curves for  ${}^7\text{Li}$ ,  ${}^9\text{Be}$ , and  ${}^{11}\text{B}$ , using low-energy ions (0 ± 20 eV energy window) normalized to the count rate for  ${}^{28}\text{Si}^{++}$  and the SiO<sub>2</sub> content of the glass, either basaltic or in NIST 61X. The linear fits to the data are forced through the origin. (Color online.)

sensitivity to singly charged ions. This might increase the reproducibility when multiply charged silicon ions are used for normalization purposes.

Although the focus of this paper is on using multiply charged ions in SIMS, we have noted that the calibration curves obtained when normalizing to singly charged silicon tend to show small matrix effects when low-energy ions are used. This is also true when ions with 75 eV initial kinetic energy are detected for

**FIGURE 4.** Calibration curves for  ${}^7\text{Li}$ ,  ${}^9\text{Be}$ , and  ${}^{11}\text{B}$ , using low-energy ions (0 ± 20 eV energy window) normalized to the count rate for  ${}^{28}\text{Si}^{+++}$  and the SiO<sub>2</sub> content of the glass, either basaltic or in NIST 61X. The linear fits to the data are forced through the origin. (Color online.)

beryllium and boron, but lithium shows a different calibration between the two matrices by 30%. This matches very closely the results presented in a more detailed study by de Hoog and EIMF (2018). They showed a linear relation between the relative ion yield (proportional to the slopes on the calibration curves presented here) and SiO<sub>2</sub> content. Because the signal intensity for the low-energy Li ions is ~300× higher than the high-energy ions, we recommend that analyses of samples with

**TABLE 2.** Comparisons of calibration curves on basaltic and high-silica glass standards

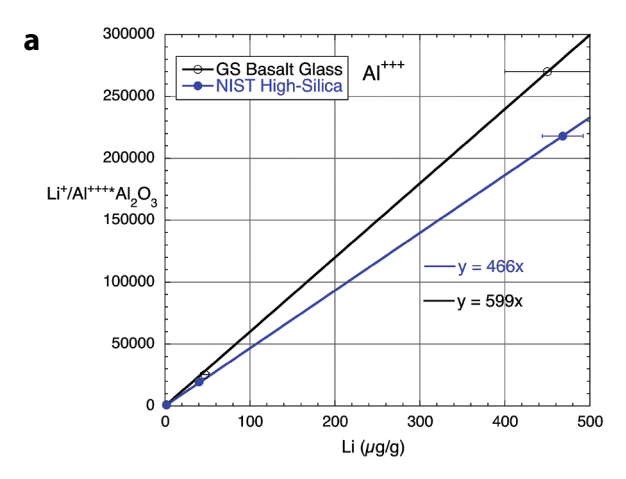
giass standards					
Date	Ratio of Basalt/NIST				
	Si+	Si <sup>++</sup>	Si***	Al***	O <sup>+</sup>
Li					
9/10/19	0.73	1.12			
11/5/19	0.92	1.50			
11/5/19	0.71	1.19			
6/29/21					
7/15/21	1.10	1.97	1.77	1.29	1.56
7/16/21	0.84	1.42	1.34	1.00	1.23
2/3/22	1.20	1.58	1.23	1.00	1.43
2/3/22	1.20	1.94	1.74	1.29	1.61
Be					
11/5/19	0.95	1.57			
11/5/19	0.96	1.58			
6/29/21	0.98		1.31	1.04	1.32
7/15/21	1.03	1.82	1.64	1.19	1.44
7/16/21	0.99	1.66	1.55	1.16	1.45
2/3/22	1.17	1.45	1.19	0.96	1.37
2/3/22	1.15	1.81	1.63	1.21	1.53
В					
9/10/19	0.92	1.40			
11/5/19	1.03	1.70			
11/5/19	0.90	1.51			
6/29/21	1.04		1.39	1.11	1.39
7/15/21	1.09	1.89	1.75	1.25	1.71
7/16/21	1.02	1.67	1.63	1.21	1.52
2/3/22	1.13	1.43	1.19	0.97	1.37
2/3/22	1.13	1.83	1.65	1.22	1.51

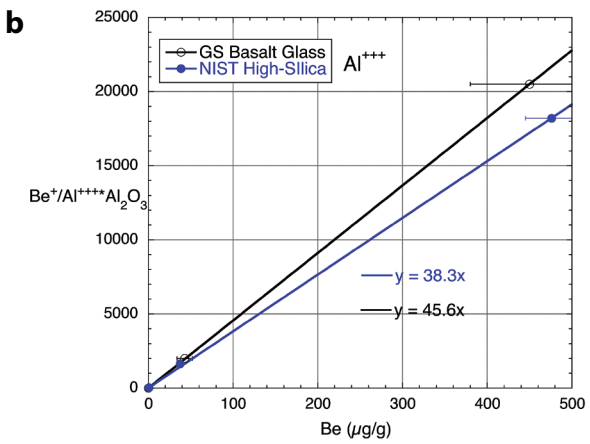
*Notes*: Italics identify sessions using secondary ions with 75 eV initial kinetic energy. All other measurements used secondary ions with  $0\pm20$  eV initial kinetic energy.

low concentrations (i.e., below  $\sim 1~\mu g/g$ ) take advantage of the combined minimal matrix effects and maximum sensitivity at these analysis conditions (intensities for Be and B low-energy ions are a bit less than  $100\times$  the intensity of 75 eV ions). Note that de Hoog and EIMF (2018) also indicated that matrix effects for Li analyses by SIMS were reduced when lower energy ions were studied.

We have frequently mentioned the collinearity of the USGS and NIST glasses in different figures, despite the relatively poor precision indicated in papers by Guillong et al. (2005) and Jochum et al. (2011). Although our analyses may fortuitously be in areas of the glass that are more representative of the average compositions than other parts of these glass samples, we can tentatively suggest that the precision in concentrations may be better than indicated. Again, the careful efforts by de Hoog and EIMF (2018) also support homogeneous Li contents in the GS glasses.

While the emphasis of this work is on light elements, we also conducted preliminary tests (using conventional energy filtering to minimize molecular ion interferences) on the effect of using Si<sup>2+</sup> as a normalizing species when quantifying selected lithophile elements (see Online Materials<sup>1</sup>). When considering Rb, Sr, Y, Zr, Ba, and Ce, the calibration curve for the USGS basaltic glasses was noticeably steeper than the slope of the curve for the NIST glasses. The effect was made much smaller if Si<sup>+</sup> was used for normalization, similar to the results on Be and B. However, the results on Pb showed large matrix effects between basaltic and the high-silica NIST glasses regardless of the choice of Si<sup>+</sup> or Si<sup>2+</sup>. In addition, examining Th and U in the two matrices showed ~25% differences in the calibration curves when normalized to Si<sup>+</sup> ions and much larger differences when using Si<sup>2+</sup> (Online Materials<sup>1</sup>).





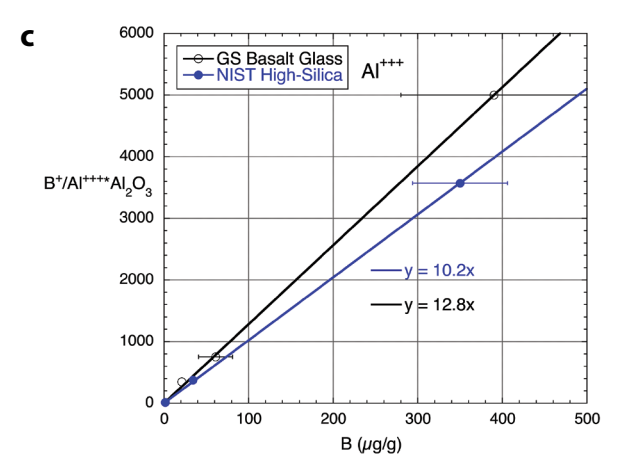


**FIGURE 5.** Calibration curves for  ${}^7\text{Li}$ ,  ${}^9\text{Be}$ , and  ${}^{11}\text{B}$ , using low-energy ions (0 ± 20 eV energy window) normalized to the count rate for  ${}^{27}\text{Al}^{+++}$  and the  $\text{Al}_2\text{O}_3$  content of the glass, either basaltic or in NIST 61X. The linear fits to the data are forced through the origin. (Color online.)

#### **IMPLICATIONS**

Using multiply charged Si ions as a normalizing ion species may lead to significant matrix effects in SIMS analysis, avoidable by using standards similar in chemistry to unknowns. Because this study examined only the NIST 61X high-silica and USGS basaltic glass compositions, it is speculative to comment on

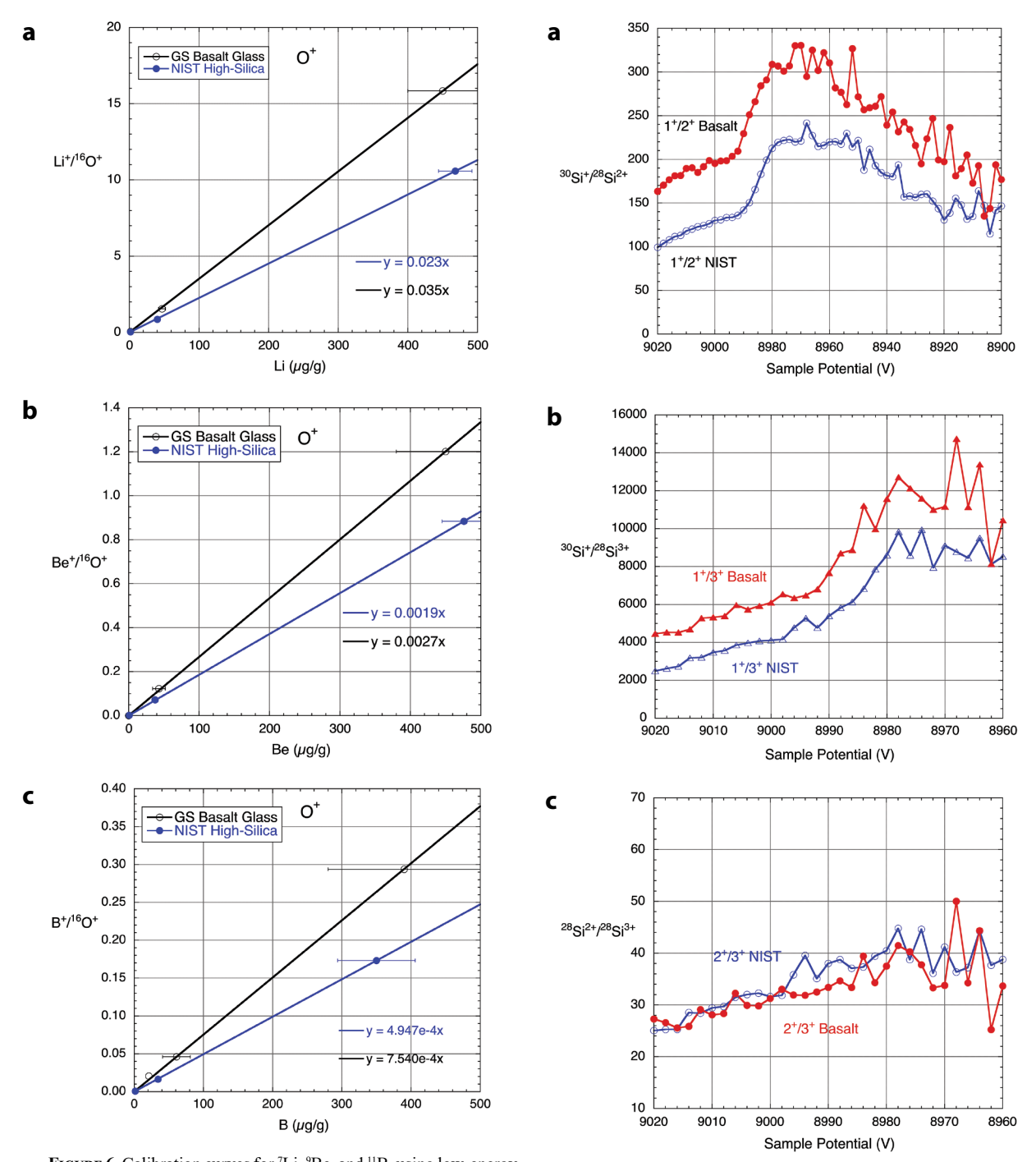


**FIGURE 6.** Calibration curves for  $^7\text{Li}$ ,  $^9\text{Be}$ , and  $^{11}\text{B}$ , using low-energy ions (0  $\pm$  20 eV energy window) normalized to the count rate for  $^{16}\text{O}^+$  from the glass, either basaltic or in NIST 61X. The linear fits to the data are forced through the origin. The primary beam was  $^{16}\text{O}_2^-$ . (Color online.)

**FIGURE 7.** Relative changes in  $Si^{x^+}$  ion intensity with sample potential (maximum signal intensity at ~9000 V). Figures described in text. Data from Figure 1. Note x-scale change for two lower figures. (Color online.)

other compositions. However, we suggest that unknowns with similar sputter yields as standards, and thus similar amounts of oxygen in the crater surface, would show the smallest matrix effects when normalizing to Si<sup>2+</sup> or Si<sup>3+</sup>. Considering the small variation in molar oxygen contents among a large number of materials commonly studied by SIMS, significant differences in

the <sup>16</sup>O<sup>+</sup> intensity between standards and unknowns may provide a warning of the matrix effect revealed in this study. Using doubly charged silicon will not negatively influence the precision of SIMS analyses if the sample matrix is unchanging, such as when conducting step scans across crystals or glasses zoned only in trace elements or in most analyses using depth profiling techniques. In fact, we have monitored the energy spectrum of <sup>28</sup>Si<sup>2+</sup> as a check on sample charging while conducting depth profiles on insulators and obtained the same overall results (diffusion coefficients) as profiles where <sup>30</sup>Si<sup>+</sup> was used for monitoring charging. Normalizing to Si<sup>+</sup> and detecting the most abundant (low-energy) secondary ions appears to minimize matrix effects (for these contrasting composition standard materials) while maximizing sensitivity.

#### ACKNOWLEDGMENTS AND FUNDING

The authors thank Lynda Williams for help with the operation of the Cameca IMS of SIMS instrument, and Peter Williams for inspiring this study with his work on multiply charged ions. We are grateful to the U.S. National Science Foundation for supporting the operation of the ASU SIMS and NanoSIMS as a multi-user community facility (currently NSF EAR 1819550) since 2007.

## REFERENCES CITED

- de Hoog, J.C.M. and EIMF (2018) Matrix effects during SIMS measurement of the lithium mass fractions of silicate glasses: correction procedures and updated preferred values of reference materials. Geostandards and Geoanalytical Research, 42, 513–522.
- Deng, R.-C. and Williams, P. (1989) Factors affecting precision and accuracy in quantitative analysis by secondary ion mass spectrometry. Analytical Chemistry, 61, 1946–1948, https://doi.org/10.1021/ac00192a035.
- Dumke, M.F., Tombrello, T.A., Weller, R.A., Housley, R.M., and Cirlin, E.H. (1983) Sputtering of the gallium-indium eutectic alloy in the liquid phase. Surface Science, 124, 407–422, https://doi.org/10.1016/0039-6028(83)90800-2.
- Dunham, E.T., Wadhwa, M., Desch, S.J., and Hervig, R.L. (2020) Best practices for determination of initial <sup>10</sup>Be/<sup>9</sup>Be in early Solar System materials by SIMS. Geostandards and Geoanalytical Research, DOI: 10.1111/ggr.12329
- Franzreb, K., Sobers, R.C. Jr., Lorincik, J., and Williams, P. (2004) Formation of doubly positively charged diatomic ions of Mo2<sup>+</sup> produced by Ar<sup>+</sup> sputtering of an Mo metal surface. The Journal of Chemical Physics, 120, 7983–7986, https://doi.org/10.1063/1.1690234.
- Guillong, M., Hametner, K., Reusser, E., Wilson, S.A., and Günther, D. (2005) Preliminary characterisation of new glass reference materials (GSA-1G, GSC-1G, GSD-1G and GSE-1G) by laser ablation-inductively coupled plasma-mass spectrometry using 193 nm, 213 nm and 266 nm wavelengths. Geostandards Newsletter, 29, 315–331, https://doi.org/10.1111/j.1751-908X.2005.tb00903.x.
- Harrison, T.M., Heizler, M.T., McKeegan, K.D., and Schmitt, A.K. (2010) In situ <sup>40</sup>K-<sup>40</sup>Ca 'double-plus' SIMS dating resolves Klokken feldspar <sup>40</sup>K-<sup>40</sup>Ar paradox. Earth and Planetary Science Letters, 299, 426–433, https://doi.org/ 10.1016/j.epsl.2010.09.023.
- Hervig, R.L. (1996) Analyses of geological materials for boron by secondary ion mass spectrometry. In E.S. Grew and L.M. Anovitz, Eds., Boron: Mineralogy, petrology, and geochemistry in the Earth's crust, 33, 789–804. Reviews in Mineralogy and Geochemistry, Mineralogical Society of America, Chantilly, Virginia
- ——(2002) Beryllium analyses by secondary ion mass spectrometry. In E.S. Grew, Ed., Beryllium: Mineralogy, petrology, and geochemistry in the Earth's crust, 50, 319–332. Reviews in Mineralogy and Geochemistry, Mineralogical Society of America, Chantilly, Virginia.
- Jochum, K.P., Willbold, M., Raczek, I., Stoll, B., and Herwig, K. (2005) Chemical

- characterization of the USGS reference glasses GSA-1G, GSC-1G, GSD-1G, GSE-1G, BCR-2G, BHVO-2G and BIR-1G using EPMA, ID-TIMS, ID-ICP-MS, and LA-ICP-MS. Geostandards Newsletter, 29, 285–302, https://doi.org/10.1111/j.1751-908X.2005.tb00901.x.
- Jochum, K.P., Weis, U., Stoll, B., Kuzmin, D., Yang, O., Raczek, I., Jacob, D.E., Stracke, A., Birbaum, K., Frick, D.A., and others. (2011) Determination of reference values for NIST SRM 610–617 glasses following ISO guidelines. Geostandards and Geoanalytical Research, 35, 397–429, https://doi.org/ 10.1111/j.1751-908X.2011.00120.x.
- Marschall, H.R. and Monteleone, B.D. (2015) Boron isotope analysis of silicate glass with very low boron concentrations by secondary ion mass spectrometry. Geostandards and Geoanalytical Research, 39, 31–46, https://doi.org/10.1111/ j.1751-908X.2014.00289.x.
- Ottolini, L. (2002) Accurate SIMS analysis of Ca in olivine based on high-energy doubly charged secondary ions. Journal of Analytical Atomic Spectrometry, 17, 280–283, https://doi.org/10.1039/b108569g.
- Ottolini, L., Bottazzi, P., and Vannucci, R. (1993) Quantification of lithium, beryllium, and boron in silicates by secondary ion mass spectrometry using conventional energy filtering. Analytical Chemistry, 65, 1960–1968, https://doi.org/10.1021/ac00063a007.
- Regier, M.E., Hervig, R.L., Myers, M.L., Roggensack, K., and Wilson, C.J.N. (2016) Analyzing nitrogen in natural and silicate synthetic glasses by secondary ion mass spectrometry. Chemical Geology, 447, 27–39, https://doi.org/ 10.1016/j.chemgeo.2016.10.019.
- Riciputi, L.R., Christie, W.H., Cole, D.R., and Rosseel, T.M. (1993) Analysis of rare earth elements in silicates by ion microprobe using doubly charged ions. Analytical Chemistry, 65, 1186–1191, https://doi.org/10.1021/ac00057a014.
- Schauer, S.N. and Williams, P. (1992) Doubly charged sputtered ions of fourth-row elements. Physical Review B: Condensed Matter, 46, 15452–15464, https:// doi.org/10.1103/PhysRevB.46.15452.
- Shimizu, N. and Hart, S.R. (1982) Applications of the ion microprobe to geochemistry and cosmochemistry. Annual Review of Earth and Planetary Sciences, 10, 483–526, https://doi.org/10.1146/annurev.ea.10.050182.002411.
- Slodzian, G. (1975) Some problems encountered in secondary ion emission applied to elementary analysis. Surface Science, 48, 161–186, https://doi.org/10.1016/0039-6028(75)90315-5.
- Zinner, E., Fahey, A.J., and McKeegan, K.D. (1986) Characterization of Electron Multipliers by Charge Distributions. In A. Benninghoven, R.J. Colton, D.S. Simons, and H.W. Werner, Eds., Secondary Ion Mass Spectrometry SIMS V. Springer Series in Chemical Physics, vol. 44, Springer, https://doi.org/ 10.1007/978-3-642-82724-2 42.

Manuscript received October 21, 2021 Manuscript accepted March 28, 2022 Accepted manuscript online April 6, 2022 Manuscript handled by Anne Peslier

### **Endnote:**

<sup>1</sup>Deposit item AM-23-38362, Online Materials. Deposit items are free to all readers and found on the MSA website, via the specific issue's Table of Contents (go to http://www.minsocam.org/MSA/AmMin/TOC/2023/Mar2023\_data/Mar2023\_data.html).